

Figure 4. Average wall temperatures for the region upstream of the secondary dilution jets. Measurements were taken at $T_{air} = 250$ °F, $T_{fuel} = 120$ °F, $P_{cmb} = 30$ psia, and $\Delta P = 3\%$.

The results indicate that the radiometer output is a measurement of the incident radiation at the gauge location. Therefore, to gain a more comprehensive picture of the radiation in the combustor, more radiometer locations are needed. In the next series of tests, the intent is to manufacture a side panel and install more radiometers in the combustor at different locations to obtain a more comprehensive picture of the incident radiation.

Infrared camera visualization experiments

At the beginning of the program, large-scale sapphire windows were purchased to allow for visualization of the IR radiation with infrared cameras in the spectral range of 1.5 to 5 μm . The intent was to obtain large-scale IR images in the combustor and also use filters to sample spectral regions that are dominated by either blackbody radiation or by radiation from major species (H_2O , CO_2 , and CO). The referee rig uses two sets of windows for visualization: (a) an inner set that is associated with the combustor and is exposed to the combustion gases, and (b) an outer set that is installed in the surrounding pressure vessel. The inner windows are relatively thinner and are exposed to a large thermal gradient and a small pressure gradient, whereas the outer windows are exposed to large pressure gradients with much lower thermal gradients. The large outer windows worked well throughout the experiments, whereas the inner windows were found to be highly susceptible to thermal cracking. Efforts were made to improve the inner-window performance by allowing more room for thermal expansion. However, the cracking was determined to be due not to constrained thermal expansion but to thermal shock within 30 s of ignition.

Visualizations were conducted with a combination of quartz inner windows and sapphire outer windows. Quartz windows are robust with respect to the thermal shock, because of the low thermal expansion coefficient, but have the disadvantage of low transmission of IR radiation. This low transmission partially obscures the visualization of the radiation in the combustor by interference from the hot inner-window surface. The effect is more pronounced at wavelengths greater than 2.5 μm . The results from the visualization using this approach showed qualitative agreement with the radiometer findings. Figure 5 shows the infrared measurements using the quartz inner windows and sapphire outer windows along with a neutral-density broadband filter. The results are qualitatively in agreement with those in Figures 3 and 4 for the radiometer and wall

thermocouples. Of note, at the highest equivalence ratio, the regions with the highest signal for the A2 and the high-aromatic fuel, compared with HEFA fuel, are shifted further downstream.

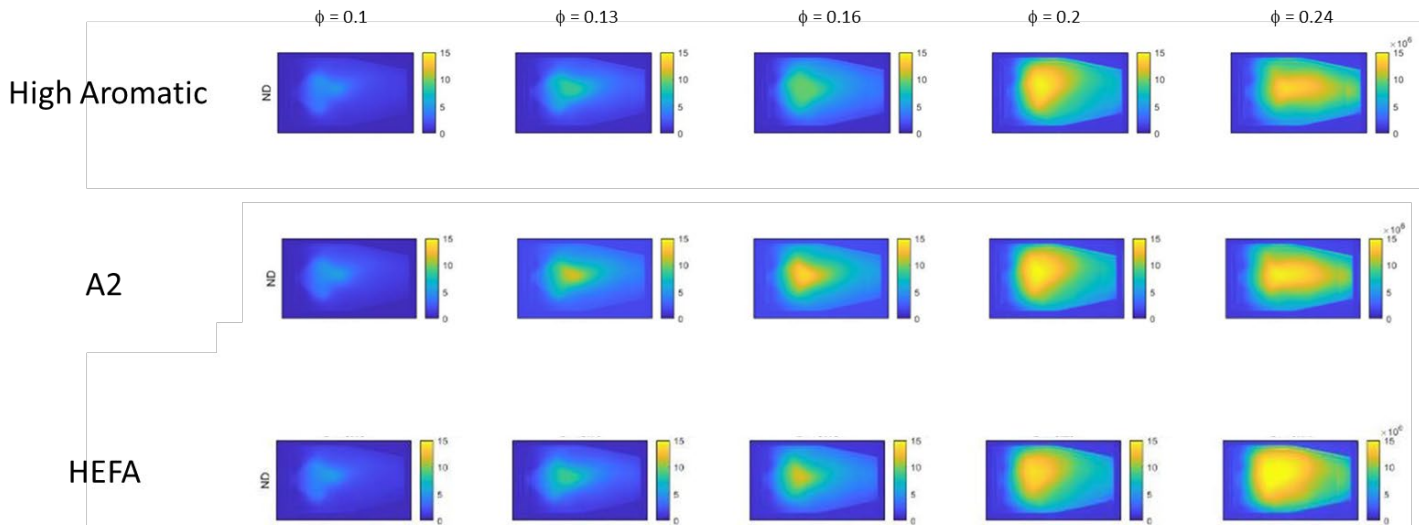


Figure 5. Infrared camera measurements for using a neutral-density filter. Measurements were taken at $T_{air} = 250 \text{ }^\circ\text{F}$, $T_{fuel} = 120 \text{ }^\circ\text{F}$, $P_{cmb} = 30 \text{ psia}$, and $\Delta P = 3\%$.

An alternative configuration for the inner window was also considered, by using thin, round port windows installed in a metallic side window. Initial experiments used a 37-mm-diameter side window and were found to be successful over a wide range of conditions. With this configuration, we were able to measure IR radiation by using spectral filters over the spectral range of the camera in proof-of-concept experiments. This window design is being extended to more port windows for subsequent experiments.

Publications

None.

Outreach Efforts

None.

Awards

None.

Student Involvement

None.

Plans for Next Period

The plans for the next period are to build on the results of the initial experiments to add more radiometers and enable IR visualization. Sampling of the combustor exhaust will also be conducted, to measure and characterize the particulate matter number density and size distribution. This second phase of experiments will include additional fuels, such as the Shell IH² high-cycloparaffin fuel. Discussions are ongoing with Shell to obtain sufficient volumes of IH² fuel for testing.



References

- Chin, J. S., & Lefebvre, A. H. (1990). Influence of fuel composition on flame radiation in gas turbine combustors. *Journal of Propulsion and Power*, 6(4), 497–503. <https://doi.org/10.2514/3.25462>
- Gleason, G.C. & Bahr, D.W. (1980). *Fuel property effects on Life Characteristics of Aircraft Turbine Engine Combustors* (Report No. 80-GT-55).
- Boehm, R., Lohmueller, S., Andac, G., Aicholtz, J., Williams, R., James, S., ... & Greene, M. (2013). Development of Combustion Rules and Tools for the Characterization of Alternative Fuels, Phase 2A. *Rept. AFRL-RQ-WP-TR-2013-0223*.
- Lefebvre, A.H. (1999). *Gas Turbine Combustion*. 2nd Edition, Taylor and Francis, Philadelphia.
- Naegeli, D.W. & Moses, C.A. (1980). *Effects of Fuel Properties on Soot Formation in Gas Turbine Engines* (Report No. 80-GT-62).
- Clark, J. A. (1982). Fuel property effects on radiation intensities in a gas turbine combustor. *AIAA Journal*, 20(2), 274–281. <https://doi.org/10.2514/3.7908>
- Rankin, B. A., Blunck, D. L., Katta, V. R., Stouffer, S. D., & Gore, J. P. (2012). Experimental and computational infrared imaging of bluff body stabilized laminar diffusion flames. *Combustion and Flame*, 159(9), 2841–2843. <https://doi.org/10.1016/j.combustflame.2012.03.022>
- Hendershott, T. H., Stouffer, S., Monfort, J. R., Diemer, J., Busby, K., Corporan, E., Wrzesinski, P., & Caswell, A. W. (2018, January 8). Ignition of conventional and alternative fuel at low temperatures in a single-cup swirl-stabilized combustor. *2018 AIAA Aerospace Sciences Meeting*. 2018 AIAA Aerospace Sciences Meeting, Kissimmee, Florida. <https://doi.org/10.2514/6.2018-1422>
- Stouffer, S., Hendershott, T., Monfort, J. R., Diemer, J., Corporan, E., Wrzesinski, P., & Caswell, A. W. (2017, January 9). Lean blowout and ignition characteristics of conventional and surrogate fuels measured in a swirl stabilized combustor. *55th AIAA Aerospace Sciences Meeting*. 55th AIAA Aerospace Sciences Meeting, Grapevine, Texas. <https://doi.org/10.2514/6.2017-1954>
- Corporan, E., Edwards, J. T., Stouffer, S., DeWitt, M., West, Z., Klingshirn, C., & Bruening, C. (2017, January 9). Impacts of fuel properties on combustor performance, operability and emissions characteristics. *55th AIAA Aerospace Sciences Meeting*. 55th AIAA Aerospace Sciences Meeting, Grapevine, Texas. <https://doi.org/10.2514/6.2017-0380>
- Esclapez, L., Ma, P. C., Mayhew, E., Xu, R., Stouffer, S., Lee, T., Wang, H., & Ihme, M. (2017). Fuel effects on lean blow-out in a realistic gas turbine combustor. *Combustion and Flame*, 181, 82–99. <https://doi.org/10.1016/j.combustflame.2017.02.035>
- Colborn, J., Heyne, J. S., Hendershott, T. H., Stouffer, S. D., Peiffer, E., & Corporan, E. (2020, January 6). Fuel and operating condition effects on lean blowout in a swirl-stabilized single-cup combustor. *AIAA Scitech 2020 Forum*. AIAA Scitech 2020 Forum, Orlando, FL. <https://doi.org/10.2514/6.2020-1883>
- Mayhew, E., Mitsingas, C. M., McGann, B., Hendershott, T., Stouffer, S., Wrzesinski, P., Caswell, A. W., & Lee, T. (2017, January 9). Spray characteristics and flame structure of jet and alternative jet fuels. *55th AIAA Aerospace Sciences Meeting*. 55th AIAA Aerospace Sciences Meeting, Grapevine, Texas. <https://doi.org/10.2514/6.2017-0148>
- Monfort, J. R., Stouffer, S., Hendershott, T., Wrzesinski, P., Foley, W., & Rein, K. D. (2017, January 9). Evaluating combustion instability in a swirl-stabilized combustor using simultaneous pressure, temperature, and chemiluminescence measurements at high repetition rates. *55th AIAA Aerospace Sciences Meeting*. 55th AIAA Aerospace Sciences Meeting, Grapevine, Texas. <https://doi.org/10.2514/6.2017-1101>
- Erdmann, T. J., Burrus, D. L., Briones, A. M., Stouffer, S. D., Rankin, B. A., & Caswell, A. W. (2017). Experimental and computational characterization of flow rates in a multiple-passage gas turbine combustor swirler. *Volume 4B: Combustion, Fuels and Emissions*, V04BT04A076. <https://doi.org/10.1115/GT2017-65252>
- Briones, A. M., Stouffer, S., Vogiatzis, K., & Rankin, B. A. (2017, January 9). Effects of liner cooling momentum on combustor performance. *55th AIAA Aerospace Sciences Meeting*. 55th AIAA Aerospace Sciences Meeting, Grapevine, Texas. <https://doi.org/10.2514/6.2017-0781>
- Stouffer, S. D., Hendershott, T. H., Colborn, J., Monfort, J. R., Corporan, E., Wrzesinski, P., & Caswell, A. (2020, January 6). Fuel effects on altitude reflight performance of a swirl cup combustor. *AIAA Scitech 2020 Forum*. AIAA Scitech 2020 Forum, Orlando, FL. <https://doi.org/10.2514/6.2020-1882>
- Stouffer, S.D., Hendershott, T.H., Boehm, R., Lovett, J. (2021). Chapter 4: The Referee Rig Combustor. Fuel effects of operability of gas turbine combustors. *Progress in Astronautics and Aeronautics*. AIAA 2021 <https://doi.org/wrs.idm.oclc.org/10.2514/5.9781624106040.0115.0142>